Phenomenological theories of ferroelectric phase transitions

W. Cao

Phenomenological theories for ferroelectrics are based on Landau–Devonshire type models, which can be constructed based on thermodynamic principles and symmetry relationships between parent and product phases. Phenomenological theories can be directly linked to measurable macroscopic quantities and at the same time preserve microscopic information. The competition between gradient energy and non-linear energy in Ginzburg–Landau type models provides an interpretation of inhomogeneous structures in ferroelectrics, for example twins and domain walls. Phenomenological models can be extended to antiferroelectric systems using a multicomponent order parameter related to microscopic local dipoles, rather than the average polarisation vector. Such a model can provide a more rigorous description of the antiferroelectric phase transition. BCT/704

Keywords: Antiferroelectrics, Dipole moments, Phase transitions, Phenomenological theory, Polarisation.

The author is at the Materials Research Laboratory, Pennsylvania State University, University Park, PA 16802, USA (cao@math.psu.edu). *Paper presented at the symposium '55 years of ferroelectrics' held in Leeds, UK on 21–23 September 2003. Manuscript accepted without revision 24 February 2004.*

INTRODUCTION

The first phenomenological model for ferroelectrics was developed by Devonshire in 1949 for $BaTiO_3$.[1] This model is an extension of the Landau theory for second order phase transitions, which utilises the fact that the amplitude of the soft mode becomes dominant in energy expansion near the phase transition temperature. The Landau theory is also applicable to weakly first order transitions. Although the soft mode never becomes totally soft in first order transitions, its amplitude can still be dominant near the phase transition. The Landau theory has been generalised to many different systems and the order parameter is no longer limited to the amplitude of the soft mode. An interesting study showed that the Landau theory is valid even for temperatures far away from the phase transition.[2] The generalised phenomenological theory is therefore much less restrictive than the original Landau theory of phase transitions. On the other hand, the procedure and symmetry constraints are still preserved in most phenomenological theories.

The primary order parameter for describing a ferroelectric system is electrical polarisation. Elastic strain plays the role of a second order parameter, which can influence phase transition, domain formation and other related physical phenomena. By including the gradient terms of the order parameter in the free energy expansion, phenomenological theory can also describe inhomogeneous structures appearing in the ferroelectric phase transition, such as twins, antiphase structures and domain walls. Here two examples will be used to show the procedure and the power of phenomenological theories in multidimensions for describing domain walls in ferroelectric systems and antiferroelectric phase transitions.

FREE ENERGY BASED ON CRYSTAL SYMMETRY

In phenomenological theories, the key quantity is the order parameter. A proper ferroelectric phase transition is driven by a zone centre transverse optical soft mode, which is related to the amplitude of the polarisation. Thus a ferroelectric system is a textbook example of the Landau theory of phase transitions.[3–5] Following Landau's ideas for a second order phase transition,[6,7] the free energy density is written in terms of a polynomial expansion of the polarisation $\boldsymbol{P}$, the volume average of the dipole moments formed during the ferroelectric phase transition.

Many well known ferroelectrics, including $BaTiO_3$, $PbTiO_3$ and PZT, have the perovskite structure. The symmetry group of the paraelectric phase for a perovskite structure is cubic mm. The ferroelectric phase transition is driven by a soft zone center Γ_4^- mode, which leads to the formation of an electric dipole in each unit cell. There are several possible low temperature phases resulting from the softening of the Γ_4^- mode, including tetragonal 4mm, orthorhombic mm2, rhombohedral 3m, monoclinic m and triclinic 1. At room temperature, however, the most commonly encountered perovskite ferroelectrics have either tetragonal 4mm symmetry or rhombohedral 3m symmetry. Here only the 4mm symmetry case is considered.

Considering a perovskite ferroelectric single crystal system, the Landau free energy density up to the sixth power in P can be written as[1,8–10]

$$\begin{aligned} f_{\mathrm{L}} = {} & \alpha_1(P_1^2+P_2^2+P_3^2)+\alpha_{11}(P_1^2+P_2^2+P_3^2)^2 \\ & +\alpha_{12}(P_1^2P_2^2+P_2^2P_3^2+P_1^2P_3^2)+\alpha_{111}(P_1^6+P_2^6+P_3^6) \\ & +\alpha_{112}[P_1^4(P_2^2+P_3^2)+P_2^4(P_1^2+P_3^2)+P_3^4(P_1^2+P_2^2)] \\ & +\alpha_{123}P_1^2P_2^2P_3^2 \quad . \quad . \quad . \quad . \quad . \quad . \quad . \quad . \quad . \quad . \quad . \quad . \quad (1) \end{aligned}$$

To account for the induced structural distortion, the elastic and electromechanical coupling energies must always be included in the phenomenological theory. The elastic energy density and the coupling energy density for a perovskite system are given by

$$\begin{aligned} f_{\mathrm{el}} = {} & c_{11}(\eta_{11}^2+\eta_{22}^2+\eta_{33}^2)/2+c_{12}(\eta_{11}\eta_{22}+\eta_{11}\eta_{33}+\eta_{22}\eta_{33}) \\ & +2c_{44}(\eta_{12}^2+\eta_{23}^2+\eta_{23}^2) \quad . \quad . \quad . \quad . \quad . \quad . \quad . \quad . \quad . \quad . \quad (2) \\ f_{\mathrm{c}} = {} & -q_{11}(\eta_{11}P_1^2+\eta_{22}P_2^2+\eta_{33}P_3^2) \\ & -q_{12}[\eta_{11}(P_2^2+P_3^2)+\eta_{22}(P_1^2+P_3^2)+\eta_{33}(P_1^2+P_3^2)] \\ & -2q_{44}(\eta_{12}P_1P_2+\eta_{13}P_1P_3+\eta_{23}P_2P_3) \quad . \quad . \quad . \quad . \quad (3) \end{aligned}$$

where $\eta_{ij}=(\partial u_i/\partial x_j+\partial u_j/\partial x_i)/2$ is the linear elastic stain tensor, c_{ij} are the elastic stiffness constants and q_{ij} the electrostriction coefficients.

DOI 10.1179/096797804225012774

Table 1 Landau free energy densities for some typical proper ferroelectrics

Parent phase	Compatible product phases (irrep.)	Free energy density
O_h	C_{4v} (Γ_4^-), C_{2v}, C_{3v}, C_s, C_1	$f_{0h} = \alpha_1 P^2 + \alpha_{11} P^4 + \alpha_{12}(P_1^2P_2^2 + P_2^2P_3^2 + P_1^2P_3^2) + \alpha_{111}P^6 + {}_{112}[P_1^4(P_2^2 + P_3^2) + P_2^4(P_1^2 + P_3^2) + P_3^4(P_1^2 + P_2^2)] + \alpha_{123}P_1^2P_2^2P_3^2$, where $P^2 = P_1^2 + P_2^2 + P_3^2$
T_h	C_{2v} (Γ_4^-), C_3, C_s, C_1	$f_{Th} = f_{0h} + \alpha_{166}(P_1^4P_2^2 + P_2^4P_3^2 + P_3^4P_1^2)$
T	C_2 (Γ_4^-), C_3, C_1	$f_T = f_{Th} + \alpha_{3T}P_1P_2P_3 + \alpha_{5T}(P_1^3P_2P_3 + P_2^3P_1P_3 + P_3^3P_1P_2)$
D_{6h}	C_{6v} (Γ_2^-)	$f_{D6h}^{(1)} = \alpha_3 P_3^2 + \alpha_{33}P_3^4 + \alpha_{333}P_3^6$
	C_{2v} (Γ_6^-), C_s	$f_{D6h}^{(2)} = \alpha_1(P_1^2 + P_2^2) + \alpha_{11}(P_1^2 + P_2^2)^2 + \alpha_{111}(P_1^2 + P_2^2)^3 + \alpha_{6D}(P_1^6 - 15P_1^4P_2^2 + 15P_1^2P_2^4 - P_2^6)$
D_{3d}	C_{3v} (Γ_2^-)	$f_{D3v}^{(1)} = \alpha_3 P_3^2 + \alpha_{33}P_3^4 + \alpha_{333}P_3^6$
	C_2 (Γ_3^-), C_m, C_1	$f_{D3v}^{(2)} = \alpha_1(P_1^2 + P_2^2) + \alpha_{11}(P_1^2 + P_2^2)^2 + \alpha_{111}(P_1^2 + P_2^2)^3 + \alpha_{a12}(P_1^6 - 3P_1^4P_2^2 + 3P_1^2P_2^4 - P_2^6)$

There are many other ferroelectric systems with symmetries other than cubic mm, and for them the free energies can be derived following the same symmetry invariant principle. For convenience, Table 1 lists symmetry invariant energy densities for several ferroelectric systems, together with the corresponding soft mode represented by the irreducible representation. Equivalent expansion forms may be found in other published sources.[11,12] In the present paper the free energy density has been truncated at the sixth power of P. If the transition is of second order, all sixth power coefficients should be set to zero.

Since there is more than one low temperature variant in the ferroelectric phase, particularly when the order parameter is multidimensional, twinning between low temperature states is unavoidable. There is a transition region between two domains in a twin structure known as a domain wall. Since the domain wall region involves electrical and elastic deformation, the energy penalty associated with the order parameter gradients must be added. Such extended phenomenological theory is usually termed Ginzburg–Landau theory because the gradient terms were first introduced by Ginzburg and Landau to describe the superconducting transition.[13] The gradient energy terms must also be invariant under the symmetry operations of the point group of the parent phase. This symmetry requirement for the gradient terms is underemphasised in the literature. In many cases, a single term proportional to the square of the polarisation gradient is used. For multidimensional anisotropic materials, more gradient invariant terms must be included. The difficulty is that there are often many invariant gradient terms for a given symmetry, which not only increases the mathematical difficulties but also makes it impossible to determine the gradient expansion coefficients experimentally. It can be verified that not all the symmetry allowed gradient invariants produce new contributions in the energy minimisation process. For example, based on the perovskite mm symmetry operations, there are seven fourth rank polarisation gradient invariants allowed, three of them combinations of $P_iP_{j,kl}$ and the other four combinations of $P_{i,j}P_{k,l}$, where the indices after a comma in the subscripts represent partial derivatives with respect to the corresponding space variables. However, in reality only three out of these seven invariants are truly independent in the sense that they will change the form of the differential equations. Thus the gradient energy for a perovskite system can be written as[10]

$$f_g = g_{11}(P_{1,1}^2 + P_{2,2}^2 + P_{3,3}^2) + g_{12}(P_{1,1}P_{2,2} + P_{1,1}P_{3,3} + P_{2,2}P_{3,3}) + g_{44}(P_{1,2}^2 + P_{1,3}^2 + P_{2,1}^2 + P_{2,3}^2 + P_{3,1}^2 + P_{3,2}^2) \quad . \quad (4)$$

It is very important to account accurately for the anisotropic nature of the polarisation gradients, as these can reveal much information about the system, such as preferred domain wall orientations, surface effects, domain wall thickness, domain wall energy and equilibrium domain size. For convenience, the gradient energies for some commonly encountered ferroelectric systems are listed in Table 2 together with the soft modes and corresponding symmetry compatible ferroelectric phases.

EQUILIBRIUM STATES AND TWINNING

After constructing the free energy, the equilibrium solution can be found by minimising the total free energy with respect to polarisation using the variational technique. The total free energy is given by

$$F = \iiint (f_L + f_{el} + f_c + f_g)\mathrm{d}v \quad . \quad (5)$$

For a ferroelectric system, the minimisation must also be performed with respect to the elastic displacement field $\boldsymbol{u}$. This leads to the Euler–Lagrange equations

$$\frac{\partial}{\partial x_j}\left(\frac{\partial f}{\partial P_{i,j}}\right)\frac{\partial f}{\partial P_i} = 0 \ (i,j = 1, 2, 3) \quad . \quad (6)$$

$$\sigma_{ij,j} = \frac{\partial}{\partial x_j}\left(\frac{\partial f}{\partial u_{i,j}}\right) = 0 \ (i,j = 1, 2, 3) \quad . \quad (7)$$

Both homogeneous and inhomogeneous solutions exist for equations (6) and (7), which can describe different structural configurations and the interrelations among different physical properties.

Table 2 Gradient invariant terms for proper ferroelectric phase transitions

Parent phase	Compatible product phases (irrep.)	Free energy density of polarisation gradients f_g
O_h	C_{4v} (Γ_4^-), C_{2v}, C_{3v}, C_s, C_1	$g_{11}(P_{1,1}^2 + P_{2,2}^2 + P_{3,32}^2) + g_{12}(P_{1,1}P_{2,2} + P_{1,1}P_{3,3} + P_{2,2}P_{3,3}) + g_{44}(P_{1,2}^2 + P_{1,3}^2 + P_{2,1}^2 + P_{2,3}^2 + P_{3,1}^2 + P_{3,2}^2)$
T_h	C_{2v} (Γ_4^-), C_3, C_s, C_1	$g_{11}(P_{1,1}^2 + P_{2,2}^2 + P_{3,3}^2) + g_{12}(P_{1,1}P_{2,2} + P_{1,1}P_{3,3} + P_{2,2}P_{3,3}) + g_{44}(P_{1,2}^2 + P_{2,3}^2 + P_{3,1}^2) + g_{66}(P_{1,3}^2 + P_{2,1}^2 + P_{3,2}^2)$
T	C_2 (Γ_4^-), C_3, C_1	$g_{11}(P_{1,1}^2 + P_{2,2}^2 + P_{3,3}^2) + g_{12}(P_{1,1}P_{2,2} + P_{1,1}P_{3,3} + P_{2,2}P_{3,3}) + g_{44}(P_{1,2}^2 + P_{2,3}^2 + P_{3,1}^2) + g_{66}(P_{1,3}^2 + P_{2,1}^2 + P_{3,2}^2)$
D_{6h}	C_{6v} (Γ_2^-)	$g_{33}P_{3,3}^2 + g_{31}(P_{3,1}^2 + P_{3,2}^2)$
	C_{2v} (Γ_6^-), C_s	$g_{11}(P_{1,1}^2 + P_{1,2}^2 + P_{2,1}^2 + P_{2,2}^2) + g_{12}(P_{1,1} + P_{2,2})^2 + g_{13}(P_{1,3}^2 + P_{2,3}^2) + g_{12}(P_{1,2}^2 + P_{2,1}^2 - 2P_{1,1}P_{2,2})$
D_{3d}	C_{3v} (Γ_2^-)	$g_{33}P_{3,3}^2 + g_{31}(P_{3,1}^2 + P_{3,2}^2)$
	C_2 (Γ_3^-), C_m, C_1	$g_{11}(P_{1,1}^2 + P_{1,2}^2 + P_{2,1}^2 + P_{2,2}^2) + g_{12}(P_{1,1} + P_{2,2})^2 + g_{13}(P_{1,3}^2 + P_{2,3}^2) + g_{12}(P_{1,2}^2 + P_{2,1}^2 - 2P_{1,1}P_{2,2}) + g_{3d}(P_{1,1}P_{2,3} + P_{1,2}P_{1,3} + P_{1,3}P_{2,1} - P_{2,2}P_{2,3})$

The homogeneous solutions minimise the Landau energy since the gradient terms all vanish. Taking for example the case of a first order $m\bar{3}m \rightarrow 4mm$ phase transition, both stable and metastable solutions can be obtained in different temperature regimes, as follows.

First, for

$$T > T_1 = T_0 + \alpha'^2_{11}/3\alpha_0\alpha_{111}$$

with

$$\alpha'_{11} = \alpha_{11} - q^2_{11}/6(c_{11}+2c_{12})$$

there is only cubic paraelectric solution with

$$P_i = 0,\ \sigma_{ij} = 0\ (i,j = 1, 2, 3) \quad . \quad . \quad . \quad . \quad . \quad . \quad . \quad . \quad . \quad . \quad (8)$$

Second, for

$$T_1 > T > T_c = T_0 + \alpha'^2_{11}/4\alpha_0\alpha_{111}$$

there are two types of solutions, stable paraelectric phase solutions with cubic symmetry

$$P_i = 0,\ \sigma_{ij} = 0\ (i,j = 1, 2, 3) \quad . \quad . \quad . \quad . \quad . \quad . \quad . \quad . \quad . \quad (9)$$

and metastable ferroelectric phase solutions with tetragonal symmetry

$$\boldsymbol{P} = (\pm P_0, 0, 0), (0, \pm P_0, 0), (0, 0, \pm P_0) \quad . \quad . \quad . \quad (10)$$

with P_0 given by

$$P_0 = \{[-\alpha'_{11} + (\alpha'^2_{11} - 3\alpha_1\alpha_{111})^{1/2}]/3\alpha_{111}\}^{1/2} \quad . \quad . \quad . \quad (11)$$

Third, for $T_c > T > T_0$, the stability of the two solutions in equations (10) and (11) is reversed, i.e. the ferroelectric tetragonal phase becomes energetically stable, while the cubic phase becomes metastable.

Fourth, for $T < T_0$, only the ferroelectric tetragonal phase exists, with the spontaneous polarisation given by equation (11) with $\alpha_1 < 0$.

The presence of metastable phases in the second and third sets of solutions is a characteristic of first order phase transitions, and will cause thermal hysteresis.

Equations (6) and (7) can also produce inhomogeneous solutions, representing twinning of different domains. For the $mm \rightarrow 4mm$ phase transition, there are both 90 and 180° twins. If strain is used as the independent variable instead of elastic displacement, its components must satisfy the elastic compatibility relations[14]

$$\varepsilon_{ikl}\varepsilon_{jmn}\varepsilon_{ln,km} = 0\ (i,j,k,l,m,n = 1, 2, 3) \quad . \quad . \quad . \quad . \quad . \quad . \quad (12)$$

where ε_{ikl} is the permutation symbol. These relations provide supplementary relationships to help uniquely determine the strain components in a defect free system.

The simplest analytical twin solution is the 180° type, in which the polarisations of the two domains on both sides of the domain wall point in opposite directions. On the other hand the 90° twin is the easiest to observe experimentally, owing to the anisotropy of the optical indices and the elastic strain difference, which can be visualised using optical and electron microscopy. The phenomenological theory uses a continuous (field) function across the domain wall to describe the polarisation variation in a twin structure.

180° twin solution

In a 180° twin, there are two domains with polarisation vectors given by $[0, 0, \pm P_0]$, and all quantities depend only on the x direction, which is perpendicular to the wall. The boundary conditions are given by

$$\lim_{x \rightarrow \pm\infty} P_3(x) = \pm P_0 \quad . \quad . \quad . \quad . \quad . \quad . \quad . \quad . \quad . \quad . \quad (13)$$

$$\lim_{x \rightarrow \pm\infty} \sigma_{ij}(x) = \lim_{x \rightarrow \pm\infty} \partial f/\partial\eta_{i,j} = 0\ (i,j = 1, 2, 3) \quad . \quad . \quad . \quad (14)$$

An analytical solution for the polarisation can be obtained that satisfies the boundary conditions[7]

$$P_3(x) = P_0 \sinh(x/\xi)/(A + \sinh^2(x/\xi))^{1/2} \quad . \quad . \quad . \quad . \quad (15)$$

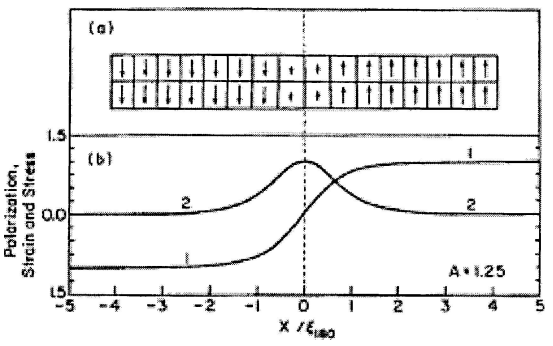

1 180° twin solution: *a* schematic illustration; *b* space profiles of polarisation (1) and normal strain deviation (2)

where

$$\xi = (g_{11})^{1/2}/P_0(6\alpha_{111}P_0^2 + 2\alpha''_{11})^{1/2} \quad . \quad . \quad . \quad . \quad . \quad . \quad (16a)$$

$$A = 3\alpha_{111}P_0^2 + \alpha''_{11}/(2\alpha_{111}P_0^2 + \alpha''_{11}) \quad . \quad . \quad . \quad . \quad . \quad . \quad (16b)$$

$$\alpha''_{11} = \alpha_{11} - q^2_{12}/2c_{11} \quad . \quad . \quad . \quad . \quad . \quad . \quad . \quad . \quad . \quad . \quad (16c)$$

The corresponding elastic strain components are

$$\eta_{11} = \eta_\perp - (q_{12}/c_{11})[P_0^2/(1 + \sinh^2(x/\xi)/A)],$$

$$\eta_{22} = \eta_\perp,\ \eta_{33} = \eta_\parallel \quad . \quad . \quad . \quad . \quad . \quad . \quad . \quad . \quad . \quad . \quad (17)$$

$$\eta_{ij} = 0\ (i,j = 1, 2, 3,\ i \neq j) \quad . \quad . \quad . \quad . \quad . \quad . \quad . \quad . \quad . \quad (18)$$

Figure 1 shows the space profile of the polarisation and the normal strain component $(c_{11}/q_{12}P_0^2)(\eta_\perp - \eta_{11})$ along x on a normalised scale. The corresponding change in polarisation vector and lattice distortion across a 180° domain wall is illustrated in Fig. 1*a*. The elastic compatibility relation in a 3D model requires the presence of inhomogeneous lateral stresses to maintain the quasi one-dimensional solutions

$$\sigma_{22} = (c_{11} - c_{12})q_{12}P_0^2/c_{11}(1 + \sinh^2(x/\xi)/A) \quad . \quad . \quad . \quad (19a)$$

$$\sigma_{33} = [q_{11} - (c_{12}/c_{11})q_{12}]P_0^2/(1 + \sinh^2(x/\xi)/A) \quad . \quad (19b)$$

It can be verified that the 180° domain wall has positive energy, which means that the multidomain state is not energetically favourable if the system is free from other constraints. However, in reality other (electrical and/or elastic) forces are always present, for example the unscreened portion of the depolarisation field, surface layer and other mechanical constraints at the boundaries of a finite system. These external forces prevent the ferroelectric system reaching a single domain state. In addition, the existence of multiple nucleation sites during phase transition produces long lived metastable multidomain configurations even without external forces. Thus the natural state of a ferroelectric crystal is generally multidomain rather than single domain.

90° twin solution

The solution of a 90° twin is a little more involved, and is described in detail in Ref. 7. Figure 2*a* illustrates the polarisation variation together with the associated elastic distortion in a 90° twin in the $z = 0$ plane. The polarisation vector rotates while changing its amplitude across the domain wall as shown in Fig. 2*b*. This solution is quasi one-dimensional, i.e. all physical quantities vary only in the direction perpendicular to the domain wall. It can be calculated that such solutions need to be sustained by inhomogeneous stresses in the wall region. Otherwise, deformation in the wall direction will occur. This deformation is the cause of the surface conjugation often observed on the surface of crystals containing 90° twins.

bct0000704 15-03-04 10:35:29 Rev 14.05
The Charlesworth Group, Huddersfield 01484 517077

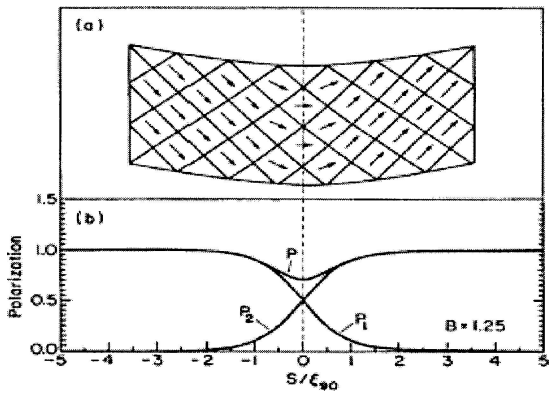

2 90° twin: *a* schematic illustration of polarisation and strain variations across twin boundary; *b* space profiles of two polarisation components and amplitude

EXTENDED THEORY FOR ANTIFERROELECTRIC SYSTEMS

The first phenomenological theory for antiferroelectric phase transition was proposed by Kittel,[15] in which were introduced two interpenetrating sublattices with equal amplitude but opposite polarisations. This model can successfully describe the double hysteresis loops observed in antiferroelectrics and can also explain the field induced antiferroelectric to ferroelectric phase transition.[15,16] However the model is not precise in the sense that it cannot specify the spatial relation between the two sublattices. In other words, the two sublattices are free to exist in space without mutual restrictions. The model also does not disclose the relationship between the unit cells of parent and product phases, for example whether cell doubling or quadrupling has occurred during the antiferroelectric phase transition. In the spirit of the Landau theory, a different multidimension order parameter can be introduced, which can successfully resolve this deficiency in the Kittel model. To be specific, ADP is used as an example.[17] The high temperature paraelectric phase of ADP is tetragonal, with space group $I\bar{4}2d$.[18–20] At $T_C \approx -125°C$, a transition to an orthorhombic antiferroelectric phase with space group $P2_12_12_1$ occurs,[19–22] accompanied by doubling of the primitive unit cell.

The transition can be described by an M point soft mode corresponding to the M_3M_4 physically irreducible representation.[12] The antiferroelectric state consists of four individual molecular dipole moments, parallel to the ***a*–*b*** plane within the unit cell of the antiferroelectric phase, as shown in Fig. 3. To describe this transition, a two component order parameter is used that corresponds to the molecular dipole at the (000) position. There are four equivalent ways of arranging the formation of these local dipoles, as shown in Fig. 4. There are therefore four distinct domains in the antiferroelectric phase, with the two component order parameter representation listed in Table 3. For convenience of

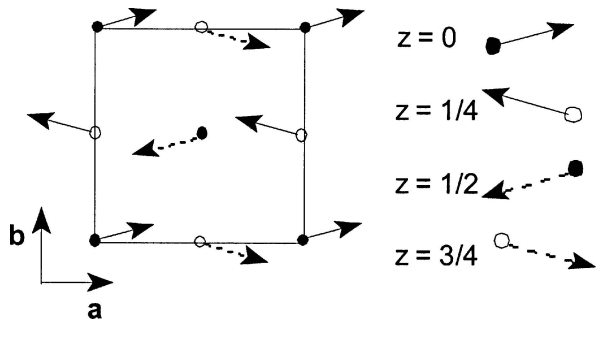

3 Dipole moments within AFE unit cell

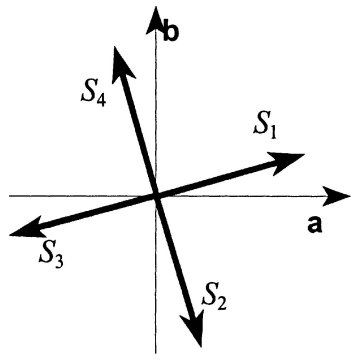

4 Directions of (000) dipole moment in four AFE domains

discussion, it is assumed that $p_a > p_b$, to ensure that the low temperature structure is orthorhombic $P2_12_12_1$.

Using such an order parameter, the free energy density can be written as

$$f = A(p_1^2 + p_2^2) + B_1(p_1^2 + p_2^2)^2 + B_2(p_1^4 + p_2^4) + B_3(p_1^3p_2 - p_1p_2^3) + C_1(p_1^2 + p_2^2)^3 + C_2(p_1^4p_2^2 + p_1^2p_2^4) + C_3(p_1^5p_2 - p_1p_2^5) + D_1\left[\left(\frac{\partial p_1}{\partial x}\right)^2 + \left(\frac{\partial p_2}{\partial y}\right)^2\right] + D_2\left(\frac{\partial p_1}{\partial x}\frac{\partial p_2}{\partial x} - \frac{\partial p_1}{\partial y}\frac{\partial p_2}{\partial y}\right) + D_3\left[\left(\frac{\partial p_1}{\partial y}\right)^2 + \left(\frac{\partial p_2}{\partial x}\right)^2\right] \quad . . . . . (20)$$

where p_1 and p_2 refer to the two components of the order parameter, i.e. the ***a*** and ***b*** components of the (000) molecular dipole moment. All coefficients are temperature independent except $A = A_0(T - T_0)$. With the addition of the order parameter gradient terms, this free energy can be used to describe the change in order parameter across a domain wall in inhomogeneous structures, such as an orientation twin or an antiphase twin.[17]

Since the space groups of the high and low temperature phases and the irreducible representations are known, the symmetry allowed distortions can be calculated based on the positions of the microscopic symmetry elements. This has been done using the Isotropy computer program,[12] and the results for the Wyckoff ***a*** sites are shown in Table 2. Using the distortions in this table, the dipole arrangement in Fig. 3 can be reproduced for any single domain state given in Table 3.

It is easy to set up a direct correlation between the microscopic order parameter used here and the macroscopic order parameter used in the Kittel model. Since polarisation

Table 3 Values of order parameter for four different domain states

Domain	Order parameter
S_1	(p_a, p_b)
S_2	$(p_b, -p_a)$
S_3	$(-p_a, -p_b)$
S_4	$(-p_b, p_a)$

Table 4 Group theoretically allowed distortions at Wyckoff *a* sites in domain S_1

Position	Distortions
(0,0,0)	p_a (1,0,0) + p_b (0,−1,0)
$(\frac{1}{2},\frac{1}{2},\frac{1}{2})$	p_a (−1,0,0) + p_b (0,1,0)
$(0,\frac{1}{2},\frac{1}{4})$	p_a (−1,0,0) + p_b (0,−1,0)
$(\frac{1}{2},1,\frac{3}{4})$	p_a (1,0,0) + p_b (0,1,0)

bct0000704 15-03-04 10:35:29 Rev 14.05
The Charlesworth Group, Huddersfield 01484 517077

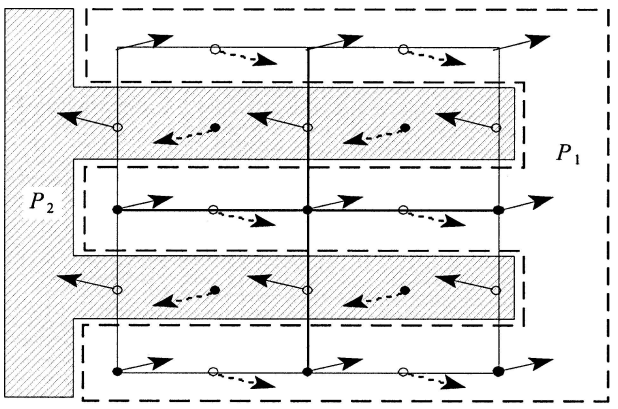

5 Definition of macroscopic Kittel sublattices in terms of microscopic dipole moments

is an average of molecular dipole moments over a given volume, the sublattice polarisations P_1 and P_2 in the Kittel model can be defined as

$$P_1 = (1/V) \sum_{\substack{i \\ (p_a > 0)}} p_{ai},\ P_2 = (1/V) \sum_{\substack{i \\ (p_a > 0)}} p_{ai} \quad . \quad . \quad . \quad . \quad (21)$$

In other words, in the antiferroelectric state, those dipole moments with a positive component in the ***a*** direction form one sublattice with effective polarisation P_1, and those with a negative component in the ***a*** direction form the other sublattice with polarisation P_2, as shown in Fig. 5. However the two sublattices depend on each other and have a fixed special relationship. The new formulation can not only derive the macroscopic Kittel model, it can also account for the spatial relationships among dipoles of adjacent cells. More importantly, it also gives the dipole tilt, which occurs in the ADP system, leading to the observed unit cell doubling associated with the antiferroelectric phase transition.

SUMMARY AND CONCLUSIONS

The thermodynamic phenomenological theory is very convenient in the sense that the parameters involved can be directly linked to measurable macroscopic quantities. At the same time, the theory also describes the microscopic symmetry changes resulting from the ferroelectric phase transition. Some studies suggest that the theory is quite accurate even out of the originally intended range of validity for the Landau theory, which makes it even more powerful for the study of phase transitions and associated phenomena. The relatively simple procedure and less involved mathematics make phenomenological theory one of the most popular models used today by both theorists and experimentalists in the study of ferroelectrics and other phase transition related phenomena.

By using generalised phenomenological theory with microscopic multidimensional order parameters, it is also possible to successfully describe the antiferroelectric phase transition. Such a formulation can not only naturally derive the Kittel model, it can also correlate the symmetries of the parent and product phases, specify the spatial relations between the two sublattices and describe the cell doubling phenomena. If the gradient terms are included in the free energy expansion, the phenomenological theories can describe many inhomogeneous structures, such as orientation twins, antiphase structures and so on, and provide polarisation space profiles inside a domain wall.

ACKNOWLEDGEMENTS

The author would like to thank former and current collaborators on phenomenological theories in ferroelectric and ferroelastic systems, including Professors G. R. Barsch, L. E. Cross, J. A. Krumhansl and D. Hatch, and Dr A. Saxena, Dr R. Hatt and Dr R. Ahluwalia.

REFERENCES

1. A. F. DEVONSHIRE: *Philos. Mag.*, 1949, **40**, 1040–1050.
2. E. K. H. SALJE: *Phys. Rep.*, 1992, **215**, 49–99.
3. W. COCHRAN: *Adv. Phys.*, 1960, **9**, 387.
4. J. TOLEDANO and P. TOLEDANO: 'The Landau theory of phase transitions'; 1987, Teaneck, NJ, World Scientific.
5. M. E. LINES and A. M. GLASS: 'Principles and applications of ferroelectrics and related materials'; 1979, Oxford, Clarendon Press.
6. L. D. LANDAU: *Phys. Z. Sowjetunion*, 1937, **11**, 26.
7. L. D. LANDAU: *Phys. Z. Sowjetunion*, 1937, **11**, 545.
8. L. E. CROSS: in 'Physics of electronic ceramics part B', (ed. L. L. Hench and D. B. Dove), 707–747; 1972, New York, NY, Marcel Dekker.
9. M. J. HAUN, E. FURMAN, S. J. JANG, H. A. MCKINSTRY and L. E. CROSS: *J. Appl. Phys.*, 1987, **62**, 3331–3338.
10. W. CAO and L. E. CROSS: *Phys. Rev. B*, 1991, **44**, 5–44.
11. G. A. SMOLENSKII *et al.*: 'Ferroelectrics and related materials'; 1984, New York, NY, Gordon and Breach.
12. H. T. STOKES and D. M. HATCH: 'Isotropy subgroups of the 230 crystallographic space groups'; 1998, River Edge, NJ, World Scientific.
13. V. L. GINZBURG and L. D. LANDAU: *Zh. Exp. Theor. Fiz.*, 1950, **20**, 1064.
14. E. A. LOVE: 'A treatise on the mathematical theory of elasticity'; 1949, New York, NY, Dover.
15. C. KITTEL: *Phys. Rev.*, 1951, **82**, 729–732.
16. L. E. CROSS: *J. Phys. Soc. Jpn*, 1967, **23**, 77–82.
17. R. HATT and W. CAO: *Phys. Rev. B*, 2000, **62**, 818–823.
18. H. MEISTER *et al.*: *Phys. Rev.*, 1969, **184**, 550–555.
19. H. KONWENT and J. LORENC: *Phys. Status Solidi (b)*, 1978, **88**, 747.
20. L. TENZER, B. C. FRAZER and R. PEPINSKY: *Acta Crystallogr.*, 1958, **11**, 505.
21. R. O. KEELING JR and R. PEPINSKY: *Z. Kristallogr.*, 1955, **106**, 236.
22. R. BLINC, J. SLAK and I. ZUPANČIK: *J. Chem. Phys.*, 1974, **61**, 988.
23. S. C. MILLER and W. F. LOVE: 'Tables of irreducible representations of space groups and co-representations of magnetic space groups'; 1967, Boulder, CO, Pruett.